Proceedings of the 24th National and 2nd International ISHMT-ASTFE Heat and Mass Transfer Conference (IHMTC-2017), December 27-30, 2017, BITS-Pilani, Hyderabad, India

IHMTC2017-19-0910

NUMERICAL INVESTIGATION OF MULTI-SPECIES UNDER-EXPANDED SONIC JETS

Apurva Bhagat *
Indian Institute of Technology, Hyderabad
me13m15p000001@iith.ac.in

Harshal Gijare
Indian Institute of Technology, Hyderabad
me13m15p000002@iith.ac.in

Nishanth Dongari
Indian Institute of Technology, Hyderabad
nishanth@iith.ac.in

ABSTRACT

We carry out numerical simulations to investigate the complex flow features in the near-field of under-expanded gas jets. OpenFOAM, an open source, computational fluid dynamics (CFD) tool is used to obtain the results. Reynolds averaged, 3 dimensional Navier-Stokes equations are solved coupled with k-Omega SST turbulence model. The new solver has been constructed to compute additional features such as transport properties of multi-species mixture based on kinetic theory. Solver is validated with the experimental and simulation data for density of a helium jet expanding in air atmosphere. We report the location and diameter of the Mach disk for helium jet and compare with the analytical results. Investigation is extended for air, argon, H_2 *and* MNH/N_2O_4 *bi-propellant fuel jet gases expanding in low pressure air atmosphere. Velocity and temperature flowfield of these gases is analyzed. Shock geometry for different jet gases is found to be weakly dependent on the specific heat ratio of jet gas medium. Location of Mach disk is farthest from nozzle exit for* H_2 *jet, and it also generates high temperature zones in the surrounding. The current study is important from the perspective of aerospace applications where sonic jets are often encountered.*

NOMENCLATURE

D_m Diameter of Mach disk
X_m Location of Mach disk
ρ Density
t Time
$\overline{u}$ Velocity of flow
Y Mass fraction
D_i Diffusion coefficient
$\dot{w}_i$ Rate of production of specie
$\overline{T}$ Viscous stress tensor
μ Dynamic viscosity
E Total energy
p Pressure
j Heat flux due to conduction
h_i Specific enthalpy of a specie
k Thermal conductivity
T Temperature
M Mach number
d Characteristic molecular diameter
Ω collision integral
C_p Specific heat at constant pressure
R Gas constant
k_B Boltmann constant
ε Characteristic energy of interaction between the molecules
X_i Mole fraction os a specie
γ Ratio of specific heat

INTRODUCTION

Sonic under-expanded jets are encountered in many applications such as exhaust plumes of rocket, reaction control jets of missile and space crafts, and accidental discharge of a gas from a high pressure cylinder. Analysis of a overall structure of jet is important to predict the risk factor in surrounding and controllability of guided space vehicles.

Figure 1 demonstrates the near nozzle flow characteristics of a sonic under-expanded jet injected in quiescent medium [1]. Jet flow undergoes Prandtl Meyer expansion near nozzle lip. These expansion waves are reflected from the jet boundary as weak compression waves and form an interception shock. These shock waves are ended by a strong normal shock which is called as the Mach disk [2]. Present work focuses on this shock characteristic for different jet gas species. It is characterized by its diameter D_m and its distance from nozzle exit X_m.

Many researchers [2–4] have performed experimental investigations of the near nozzle shock structure of under-expanded jets using wind tunnel, Schlieren and shadowgraph photography, Rayliegh scattering etc. Several types of scaling laws for velocity, temperature and mass concentration have been developed [4–6]. Numerical investigation of under-expanded air/nitrogen jets have been carried out using Euler's equations [7, 8], RANS and LES methods [9–11]. However, there exists scarcity of quantitative data of near-field properties of different jet gas species in the literature.

*Corresponding author

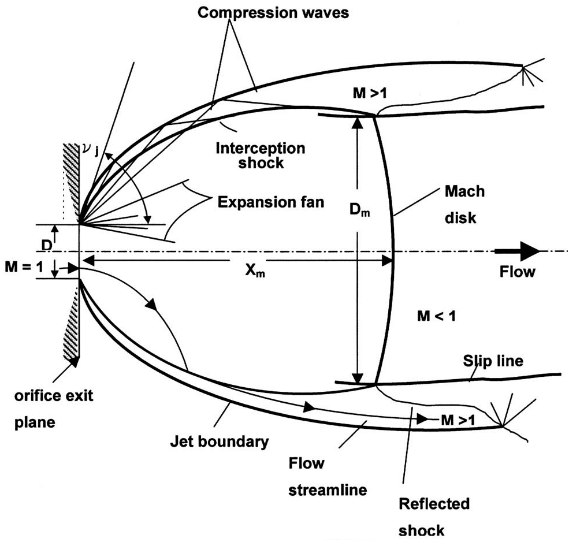

Figure 1: FLOW STRUCTURE OF A SONIC UNDER-EXPANDED JET [1].

Major objective of the paper is to perform 3 dimensional simulations of highly under-expanded multi-species jets injected in quiescent air atmosphere. In this paper, a solver is validated against experimental data, numerical data and analytical co-relations for X_m and D_m. Also, a numerical analysis of a flow structure of jet gases (Ar, He, H_2, air and MNH/N_2O_4 bi-propellant fuel) with different specific heat ratios is performed.

GOVERNING EQUATIONS

The *hypersonicIithFoam* solver is constructed by modifying the existing *rhoCentralFoam* solver [12,13] and a mass transport library [14]. It is incorporated with additional features, such as species transport, chemical kinetics and thermodynamic properties based on JANAF model. The kinetic transport model for thermal conductivity and viscosity is combined with the shock capturing capability and non-oscillatory numerical schemes of *rhoCentralFoam*. Following governing equations are solved by the solver [15].

Conservation of total mass:

$$\frac{\partial \rho}{\partial t} + \nabla \cdot [\rho \overline{u}] = 0, \tag{1}$$

Conservation of species mass:

$$\frac{\partial \rho Y_i}{\partial t} + \nabla \cdot [\overline{u} \rho Y_i] - \nabla \cdot [\rho D_i \nabla Y_i] - \dot{w}_i = 0, \tag{2}$$

Conservation of momentum:

$$\frac{\partial (\rho \overline{u})}{\partial t} + \nabla \cdot [\overline{u}(\rho \overline{u})] + \nabla p + \nabla \cdot \overline{T} = 0, \tag{3}$$

where,

$$\overline{T} = \mu \left(\nabla \overline{u} + (\nabla \overline{u})^T - \frac{2}{3} \nabla \cdot \overline{u} \right), \tag{4}$$

Conservation of energy:

$$\frac{\partial (\rho E)}{\partial t} + \nabla \cdot [\overline{u}(\rho E)] + \nabla \cdot [\overline{u} p] + \nabla \cdot [\overline{T} \cdot \overline{u}] + \nabla \cdot j - \nabla \cdot \left[\rho \sum_i h_i D_i \nabla Y_i \right] = 0, \tag{5}$$

where,

$$j = -k \nabla T, \tag{6}$$

Laminar viscosity of the individual specie i is calculated as:

$$\mu_i = 2.6693 \times 10^{-5} \frac{\sqrt{M_i T}}{d^2 \Omega_\mu}, \tag{7}$$

Thermal conductivity of an individual specie i is calculated by Eucken's relation:

$$k_{eff_i} = \mu_{eff_i} \left(C_p + \frac{5}{4} R \right), \tag{8}$$

Mixture values of μ and k are calculated as the weighted average of μ_{eff_i} and k_{eff_i} based on the mole fraction of species. Binary diffusion coefficient for specie i diffusing in specie j is calculated using Chapman-Enskog model:

$$D_{ij} = 10.1325 \frac{0.001858 T^{1.5} \sqrt{\frac{1}{M_i} + \frac{1}{M_j}}}{p d_{ij}^2 \Omega_{d,ij}}, \tag{9}$$

where d_{ij} is approximated as :

$$d_{ij} = \frac{1}{2}(d_i + d_j), \tag{10}$$

Values for $\Omega_{d,ij}$ as a function of $k_B T / \varepsilon_{ij}$ are given in [16], where $\varepsilon_{ij} = \sqrt{\varepsilon_i \varepsilon_j}$. Multicomponent diffusion coefficient D_{im}, for diffusion of specie i into mixture , is calculated as:

$$D_{im} = \frac{1 - X_i}{\sum_j \frac{X_j}{D_{ij}}}, \tag{11}$$

COMPUTATIONAL MODELING

Problem Setup

Dubois *et al.* [17] have performed a set of experiments using the BOS (Background Oriented Schlieren) technique, where the density data of the subsonic and supersonic helium jet was reported. Velikorodny *et al.* [18] developed a numerical model (*CAST3M* code) to validate these results and developed a scaling law based on dimensional analysis. According to them, for the special case of a sonic jet, shock geometry of jet can be characterized by following semi-empirical relations:

$$\frac{X_m}{D_e} = \frac{1}{2}\sqrt{\gamma}\sqrt{\frac{P_e}{P_\infty}} \times \left(\frac{\gamma+1}{\gamma-1}\right)^{\frac{1}{4}} \tag{12}$$

$$\frac{D_m}{D_e} = kX_m\sqrt{1-\frac{\gamma+1}{\gamma}\times\left(\frac{\gamma+1}{\gamma-1}\right)^{\frac{-1}{2}}} \tag{13}$$

where, k is an empirical constant which accounts for the growth of the mixing layer. It is approximated for different jet gas species, using experimental measurements. These relations suggest that location and diameter of Mach disk depends on γ and pressure ratio.

The *hypersonicIithFoam* solver is validated against Dubois experimental data [17] and *CAST3M* code [18]. Values of X_m and D_m are obtained for He jet gas and compared with the semi-empirical relations.

Computational Domain and Boundary Conditions

Figure 2 demonstrates the computational domain considered for simulations. Jet is assumed to release from 30 bar pressure tank. Region from the nozzle exit is modeled, where jet flow is in sonic condition (M_e = 1). Ambient flow-field has air with p = 101325 Pa and T = 300 K. Diameter of nozzle is D_e = 0.01 m. Reynolds number based on this diameter is above 10^6, so turbulence is modeled using k - omega SST turbulence model. Dimensions of base, height and top boundaries are $10D_e$, $35D_e$ and $48D_e$, respectively. A 3 dimensional structured mesh is generated using ICEM-CFD. It consists on 3.2 million hexahedral cells and is finer near the nozzle exit. Grid independence study has been performed by gradually refining mesh in all directions and the solution is grid independent. Each test case is simulated in parallel on 32 Intel Haswell cores on the HPC facility at IIT Hyderabad.

RESULTS AND DISCUSSIONS

Solver Validation

Validation study is performed for a sonic helium jet injected in air atmosphere. Exit velocity of helium jet is 892 m/s. Fig. 3 demonstrates the comparison of normalized density values across the centerline of jet. Density is normalized by its ambient value. It can be observed that jet density reduces rapidly along the centreline as jet is under-expanded. It experiences normal shock (also can be referred as Mach disk) at Z/D_e = 3.5. Solutions of *hypersonicIithFoam* and *CAST3M* code are in good agreement with each other, however, experimental density values are higher. These deviations with the experimental data may be due to the unsteady behavior of the jet gas, aerodynamic jet noise and uncertainties in turbulence.

Figure 4 shows the density distribution along the transverse axis at $Z = 17D_e$. Density values are low in the jet area and abruptly increase around the jet boundary. All three solutions are in good agreement with each other.

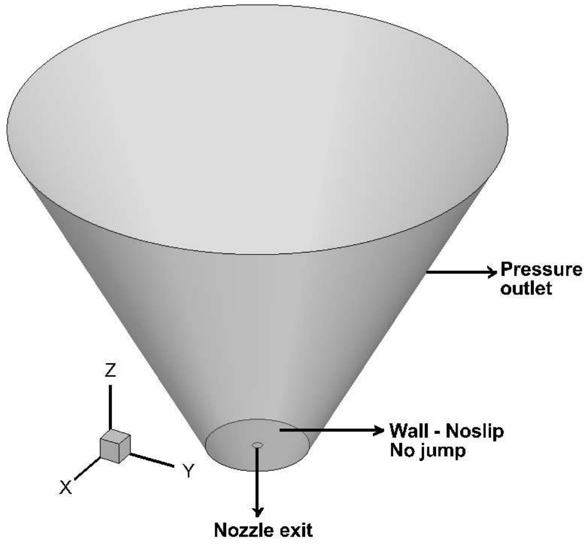

Figure 2: COMPUTATIONAL DOMAIN AND BOUNDARY CONDITIONS.

Table 1 compares the values of Mach disk location and its diameter obtained by different methods. It is observed that *hypersonicIithFoam* solver predicts X_m/D_e values accurately (within 2 % deviation with experimental and analytical solution). D_m/D_e values agree with experimental and analytical solutions with $\pm$ 8 % deviation.

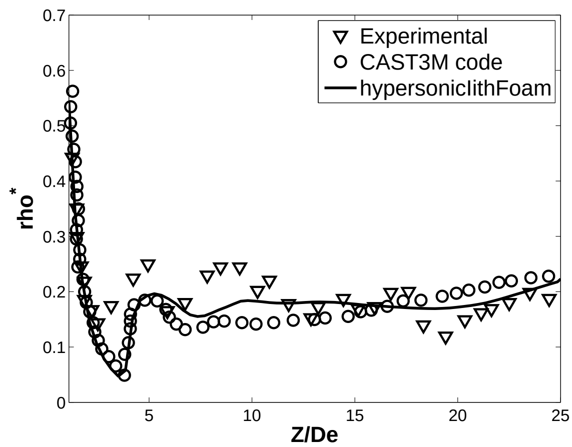

Figure 3: COMPARISON OF NORMALIZED DENSITY ALONG THE CENTERLINE OF JET.

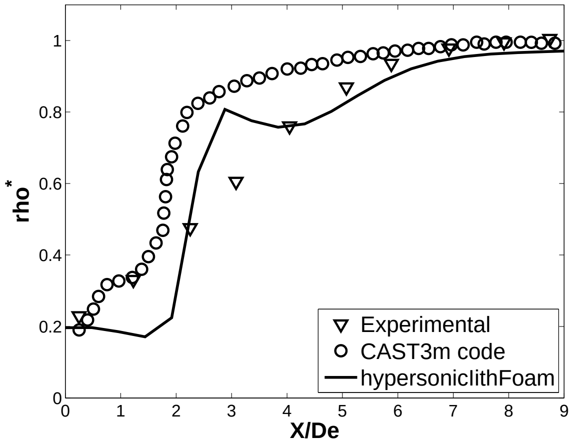

Figure 4: COMPARISON OF NORMALIZED DENSITY ALONG THE TRANSVERSE AXIS AT Z = 17 D_e.

Table 1: MACH DISK LOCATION AND DIAMETER VALUES OBTAINED BY DIFFERENT METHODS FOR HELIUM JET.

	Experimental	Eqn.s (12) and (13)	CAST3M code	hypersonic-IithFoam-
X_m/D_e	3.5 - 3.8	3.58	3.64	3.5
D_m/D_e	1.25 - 1.75	2.09	2.1	1.91

Simulations of different jet gases

Simulations are run up-to time = 0.001 seconds for air, Ar, H_2, He and MNH/N_2O_4 bi-propellant fuel jet gases. First four simulations are run by assuming 2 specie mixture in chemical and thermal equilibrium. However, MNH/N_2O_4 bi-propellant fuel jet is modeled using a set of 11 species (CO, CO_2, H, H_2, H_2O, N, NO, N_2, O, OH and O_2). Species concentration at the nozzle exit is obtained from the reference [19]. This fuel is used in divert and attitude control jets of the THAAD missile [19]. In outer atmosphere, jets would expand rapidly and may cause contamination of the space-craft surface reducing its life. In such cases, quantitative knowledge of the temperature, velocity and mass concentration of the jet gas is important.

Table 2 specifies the flow properties that affect the jet flow. It should be noted that, fuel properties are calculated by applying mixture rules to individual species properties. Fig. 5 show the normalized velocity contours for all jet gases. Velocity is normalized by sonic exit velocity U_e for each jet gas. Flow properties such as Prandtl Meyer expansion fan, Mach disk and subsonic core are qualitatively captured by *hypersonicIithFoam*. He jet being lighter specie, has high exit velocity and travels more distance compared to other jets. Mach disk location is weakly dependent on γ, as it is observed at the same location for He, Ar, Air and fuel jet. However, H_2 jet gas is observed to behave differently compared to other jet gases. Its Mach disk location is far from the nozzle exit compared to other jet gases. This can be better visualized in fig. 6. This is may be due to the fact that H_2 gas is highly flammable in air and possess entirely different thermo-physical properties from other inert gases. Strength of the normal shock is maximum for MNH/N_2O_4 bi-propellant fuel jet as it reaches 2.5 times the velocity of sound.

Table 2: Flow properties of jet gas species.

jet gas	Air	Ar	H_2	He	Fuel
γ	1.4	1.66	1.41	1.667	1.25
R (J/Kg K)	287	208	4210	2077	407.17
U_e(m/s)	304.5	282.87	1157.83	892	342.71

Figure 7 presents normalized temperature contours for all the jet gas species and fig. 8 demonstrates the quantitative data of same along the center-line of jet. Temperature is normalized by its ambient value. It is observed that temperature is maximum in the mixing layer of He jet. He jet has high kinetic energy, and when it interacts with steady atmospheric air, kinetic energy is converted into thermal energy by raising the temperature of air molecules above its ambient value. Temperature downstream of H_2 jet is also higher than the ambient. This is because of the pressure waves from jet compress the air downstream and temperature rises. Temperature profile of Fuel jet is nearly identical to that of air jet.

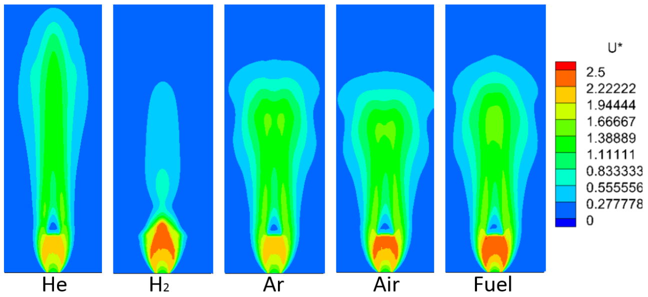

Figure 5: NORMALIZED VELOCITY CONTOURS FOR DIFFERENT JET GAS SPECIES.

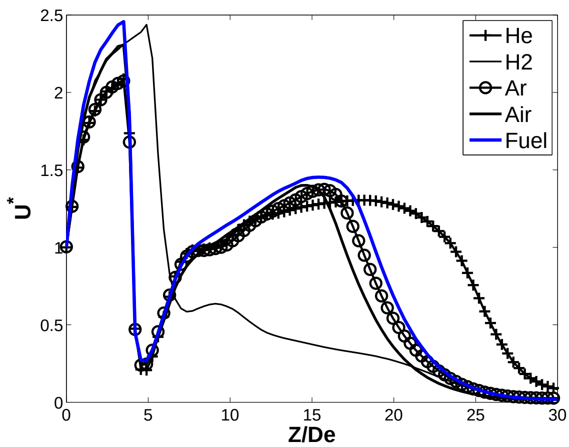

Figure 6: NORMALIZED VELOCITY PROFILE ALONG CENTERLINE FOR DIFFERENT JET GAS SPECIES.

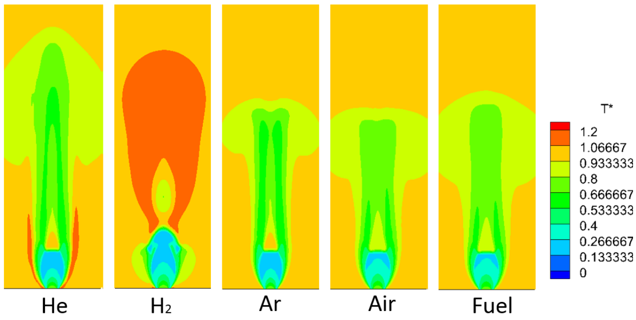

Figure 7: NORMALIZED TEMPERATURE CONTOURS FOR DIFFERENT JET GAS SPECIES.

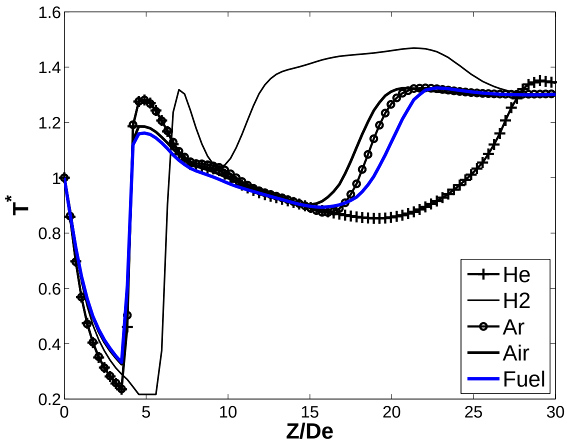

Figure 8: NORMALIZED TEMPERATURE PROFILE ALONG CENTERLINE FOR DIFFERENT JET GAS SPECIES.

Figs. 9 and 10 shows the normalized velocity and temperature profile respectively, along the transverse axis at Z = 3.5D$_e$. Z = 3.5D$_e$ location is chosen, as it is just behind the Mach disk for most of the jet gases. It is observed that Fuel jet has maximum horizontal spread and higher normalized velocity when compared to other jet gases. Temperature profiles of all jet gases show minimum temperature in the jet core, which is expected as all jets are under-expanded. He jet profile has 2 local maximums at the jet boundary as explained earlier. However, H_2 jet has minimum temperature value as its Prandtl Meyer expansion fan is wider than other jets.

CONCLUSION

A new solver is constructed to model 3 dimensional, compressible, multi-species flow. This solver extends the applicability of CFD to high altitude conditions (up-to the transition flow regime) and high temperature flows ($T \sim 8000$ K). It is validated against experimental and CAST3M code data, for density values of He jet injected in air atmosphere. Location and diameter of a Mach disk is accurately captured by *hypersonicIithFoam* when compared with analytical relations from literature.

A numerical analysis is carried out to observe different jet gas behavior. Velocity and temperature field of air, Ar, H_2, He and MNH/N_2O_4 bi-propellant fuel jet is compared. Location and diameter of Mach disk is weakly dependent on γ and is similar

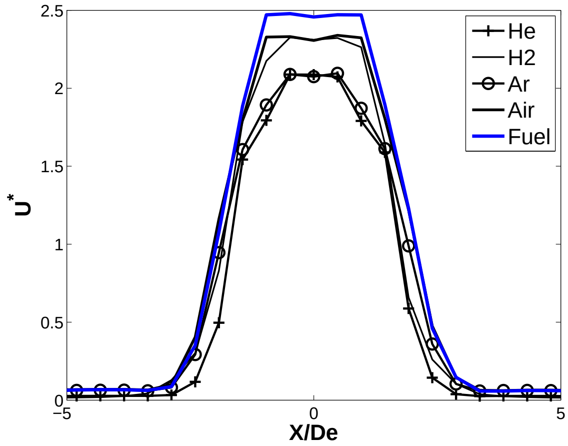

Figure 9: NORMALIZED VELOCITY PROFILE ALONG TRANSVERSE AXIS AT Z = 3.5D$_e$ FOR DIFFERENT JET GAS SPECIES.

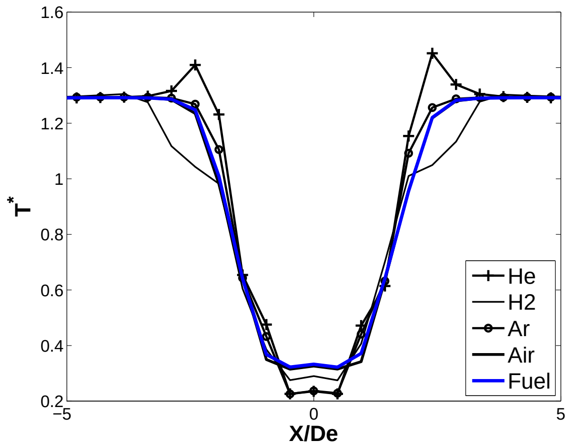

Figure 10: NORMALIZED TEMPERATURE PROFILE ALONG TRANSVERSE AXIS AT Z = 3.5D$_e$ FOR DIFFERENT JET GAS SPECIES.

for air, He, Ar and fuel jet. Position of Mach disk is considerably far from nozzle exit for H_2 jet and high temperature zone is observed. This leads to the conclusion that flow features of sonic under-expanded jet also depend on temperature dependent thermo-physical properties of jet gas.

The present work is helpful in the thermal designing of space-craft surfaces and industrial applications where accidental discharge of gases may take place. An exhaust gas plume with chemically reacting species would be considered for future work.

ACKNOWLEDGMENTS

The research is supported by DST:SERB/F/2684/2014-15 and MHRD fellowship.

REFERENCES

[1] Wu, J.-S., Chou, S.-Y., Lee, U.-M., Shao, Y.-L., and Lian, Y.-Y., 2005. "Parallel dsmc simulation of a single under-expanded free orifice jet from transition to near-continuum

regime". *Journal of fluids engineering, 127*(6), pp. 1161–1170.

[2] Crist, S., Sherman, P., and Glass, D., 1966. "Study of the highly underexpanded sonic jet". *AIAA J, 4*(1), pp. 68–71.

[3] Snedeker, R. S., et al., 1971. "A study of free jet impingement. part 1. mean properties of free and impinging jets". *Journal of fluid Mechanics, 45*(2), pp. 281–319.

[4] Ewan, B., and Moodie, K., 1986. "Structure and velocity measurements in underexpanded jets". *Combustion Science and Technology, 45*(5-6), pp. 275–288.

[5] Birch, A., Brown, D., Dodson, M., and Swaffield, F., 1984. "The structure and concentration decay of high pressure jets of natural gas". *Combustion Science and technology, 36*(5-6), pp. 249–261.

[6] Yüceil, K. B., and Ötügen, M. V., 2002. "Scaling parameters for underexpanded supersonic jets". *Physics of Fluids, 14*(12), pp. 4206–4215.

[7] Prudhomme, S., and Haj-Hariri, H., 1994. "Investigation of supersonic underexpanded jets using adaptive unstructured finite elements". *Finite elements in analysis and design, 17*(1), pp. 21–40.

[8] Irie, T., Yasunobu, T., Kashimura, H., and Setoguchi, T., 2003. "Characteristics of the mach disk in the underexpanded jet in which the back pressure continuously changes with time". *Journal of Thermal Science, 12*(2), pp. 132–137.

[9] Chauvet, N., Deck, S., and Jacquin, L., 2007. "Numerical study of mixing enhancement in a supersonic round jet". *AIAA journal, 45*(7), p. 1675.

[10] Dauptain, A., Cuenot, B., and Gicquel, L., 2010. "Large eddy simulation of stable supersonic jet impinging on flat plate". *AIAA journal, 48*(10), p. 2325.

[11] Hamzehloo, A., and Aleiferis, P., 2014. "Large eddy simulation of highly turbulent under-expanded hydrogen and methane jets for gaseous-fuelled internal combustion engines". *International Journal of Hydrogen Energy, 39*(36), pp. 21275–21296.

[12] Kurganov, A., and Tadmor, E., 2000. "New high-resolution central schemes for nonlinear conservation laws and convection–diffusion equations". *Journal of Computational Physics, 160*(1), pp. 241–282.

[13] Kurganov, A., Noelle, S., and Petrova, G., 2001. "Semidiscrete central-upwind schemes for hyperbolic conservation laws and hamilton–jacobi equations". *SIAM Journal on Scientific Computing, 23*(3), pp. 707–740.

[14] Novaresio, V., García-Camprubí, M., Izquierdo, S., Asinari, P., and Fueyo, N., 2012. "An open-source library for the numerical modeling of mass-transfer in solid oxide fuel cells". *Computer Physics Communications, 183*(1), pp. 125–146.

[15] Blazek, J., 2015. *Computational fluid dynamics: principles and applications*. Butterworth-Heinemann.

[16] Anderson, J. D., 2000. *Hypersonic and high temperature gas dynamics*. Aiaa.

[17] Dubois, J., 2010. "Etude expérimentale de jets libres, compressibles ou en présence d'un obstacle". PhD thesis, Aix-Marseille Université.

[18] Velikorodny, A., and Kudriakov, S., 2012. "Numerical study of the near-field of highly underexpanded turbulent gas jets". *international journal of hydrogen energy, 37*(22), pp. 17390–17399.

[19] Chamberlain, R., Dang, A., and McClure, D., 1999. "Effect of exhaust chemistry on reaction jet control". *AIAA paper*(99-0806).